Oral presentation | Higher order methods
Higher order methods-I
Mon. Jul 15, 2024 4:30 PM - 6:30 PM Room C

[3-C-03] A consistent viscous discretization approach using Staggered Update Procedure (SUP)

*Shubhashree Subudhi[1], N. Balakrishnan[1] (1. Indian Institute of Science, Bangalore, India)

Keywords: Higher order finite volume method, Staggered Update Procedure (SUP), Defect correction strategy, Green-Gauss procedure, Unstructured meshes

Twelfth International Conference on
Computational Fluid Dynamics (ICCFD12),
Kobe, Japan, July 14-19, 2024

A consistent viscous discretization approach using Staggered Update Procedure (SUP)

Shubhashree Subudhi* and N. Balakrishnan*
Corresponding author: nbalak@iisc.ac.in
* Indian Institute of Science, Bangalore 560012, India.

Abstract: To achieve a consistent finite volume discretization, the interfacial fluxes must be accurate at least to second order. The unstructured mesh based finite volume solvers currently employed in routine industrial computations use arbitrary volumes exhibiting high skewness. These solvers use second order accurate convective interfacial fluxes obtained through linear solution reconstruction, while the viscous fluxes are still formally first order accurate. In this paper, a Staggered Update Procedure (SUP) in the context of a consistent and higher order accurate finite volume method is presented. In contrast to the classical finite volume method wherein the vertex values are interpolated to required accuracy, an independent vertex update based on meshless method is introduced. The convective fluxes are determined to second order accuracy at the flux computing interfaces with the use of linear solution reconstruction. On the other hand, in order to determine the viscous fluxes to the same order of accuracy as that of the convective fluxes, when used with a linear reconstruction step, a novel defect correction strategy in relation to Green-Gauss procedure is developed. The benefits of the proposed SUP methodology is established through an unsteady laminar flow past a circular cylinder in 2D.

Keywords: Staggered Update Procedure (SUP), Higher order Finite Volume Method, Meshless solver, LSFD-U, Defect correction, Green-Gauss procedure, Unstructured mesh, Unsteady flow.

1 Introduction

The most widely used CFD flow solvers for aeronautical applications are based on the solution of Reynolds-Averaged Navier Stokes (RANS) equations. Most of the production codes using finite volume methodology employing linear solution reconstruction are formally first order accurate on unstructured meshes. Nevertheless, these solvers have earned the confidence of designers and engineers, and have been used extensively in the last two decades in solving several problems of industrial relevance owing to, (i)their general applicability in terms of handling complex geometries, (ii)their robustness in terms of both residual and iterative convergence, and (iii)the computational cost, in other words, the efficiency in providing reliable design data within shorter turnaround times.

For many aeronautical applications, such as flow past high-lift configurations, aeroacoustic noise prediction, high angle of attack wing flows, rotor blade flows, hypersonic flows around space vehicles, and internal flows encountered in propulsion systems, accurate computation of flow field is crucial. However, widely available RANS based solvers face limitations in predicting turbulent, separated flows, and are believed to break down in such scenarios. Hence, developing a robust, higher order accurate numerical flow solver for industrial computation has been an active research area within CFD community. The demand for such methods have has further increased with the significant advancements in the HPC technology and the use of higher fidelity CFD methods such as LES, DES, hybrid RANS/LES approaches becoming more common, in the recent years. Our work on Staggered Update Procedure (SUP) is an attempt to achieve higher order accuracy on unstructured meshes without losing robustness.

The essential idea of SUP is to update solution variables not just at cell centres, but also at the cell vertices. This is at variance with the classical finite volume method, where the vertex values are interpolated to a required accuracy. The concept of SUP was originally proposed by Shende and Balakrishnan [1] in the context of rotated difference scheme [2]. In this work, it was brought out that the solutions thus obtained exhibited significant dependence on the way the solution is interpolated at the vertices, clearly underlining the importance of accurate vertex value interpolation. It is in this context SUP, where an independent update is employed at the vertices, was proposed. We have adopted Upwind - Least Squares Finite Difference (LSFD-U) [3] procedure for solution update at vertices. LSFD-U is a generalized finite difference method that only utilize point clouds to discretize the partial differential equations and do not involve any spatial integration like in FVM, hence, they are relatively easy to

implement. The objective here is to exploit the solution available at the vertices in arriving at a higher order solution procedure on unstructured meshes.

Interestingly, much of the literature on the development of higher order unstructured mesh-based finite volume schemes has predominantly focused on the discretization of convective fluxes, with limited attention given to viscous flux discretization (with the exception of works like [4, 5, 6, 7]). This imbalance directly impacts the accuracy of the solution and its rate of convergence. Hence, there is a gap for higher order accurate viscous discretization. We would like to address this issue in particular and explore the benefits, if there are any at all, in determining the viscous fluxes to the same order of accuracy as the convective fluxes. To accomplish a higher order accurate discretization for viscous fluxes, at least to the commensurate accuracy of convective fluxes, second order accurate gradients at finite volume faces are essential.

The Green-Gauss based framework given by Jawahar and Kamath [8] for computing interfacial gradients is known to be robust and performs well, in terms of accuracy. Although this procedure recovers second order accuracy on uniform Cartesian grids, the accuracy degenerates on irregular mesh elements, which is often encountered in practical scenarios due to geometric complexities. In order to meet the accuracy constraint under such conditions, we developed a defect correction strategy [9] aimed at achieving genuinely second order accuracy of gradients at volume interfaces, while adhering to the Green-Gauss based gradient finding procedure. Consequently, the second order accuracy of interfacial gradients as well as centroidal and nodal gradients are obtained through an iterative procedure.

In our earlier work [10], we have demonstrated the superior accuracy of SUP by solving model problem for a low Peclet number. Subsequently, the extension of this methodology to flow governing equations is established in [11, 12]. A systematic grid convergence study was conducted by considering the laminar flow past NACA 0012 airfoil. Furthermore, the benefits of consistent viscous discretization was brought out by obtaining solutions on a coarse mesh. The current paper begins by reviewing the Navier-Stokes equations, followed by the details of discretisation of SUP methodology. An unsteady laminar flow past a circular cylinder corresponding to a low Reynolds number is investigated in this paper. The higher accuracy and reduced numerical diffusion of SUP is established by comparing the finite volume results obtained on a very fine structured mesh.

2 Governing Equations

The non-dimensional, unsteady compressible Navier-Stokes equations in conservative form can be expressed as,

$$\frac{\partial \mathbf{w}}{\partial t} + \boldsymbol{\nabla} \cdot [(\mathbf{f}^{con} + \mathbf{f}^{vis}) \;\; (\mathbf{g}^{con} + \mathbf{g}^{vis})] = 0 \tag{1}$$

In the above equation, $\mathbf{w} = [\rho \;\; \rho u \;\; \rho v \;\; e]^T$ is the vector of conserved variables. The inviscid flux vectors are given as, $\mathbf{f}^{con} = [\rho u \;\; \rho uu + p \;\; \rho uv \;\; (e+p)u]^T$ and $\mathbf{g}^{con} = [\rho v \;\; \rho uv \;\; \rho vv + p \;\; (e+p)v]^T$. The viscous flux vectors are written as, $\mathbf{f}^{vis} = [0 \;\; -\tau_{xx} \;\; -\tau_{xy} \;\; -(u\tau_{xx} + v\tau_{xy} - q_x)]^T$ and $\mathbf{g}^{vis} = [0 \;\; -\tau_{xy} \;\; -\tau_{yy} \;\; -(u\tau_{xy} + v\tau_{yy} - q_y)]^T$. The normal and shear stresses and heat conduction terms in viscous fluxes are given as,

$$\tau_{xx} = \frac{\mu}{Re_\infty}\left(2\frac{\partial u}{\partial x} - \frac{2}{3}\left(\frac{\partial u}{\partial x} + \frac{\partial v}{\partial y}\right)\right), \;\; \tau_{xy} = \frac{\mu}{Re_\infty}\left(\frac{\partial u}{\partial y} + \frac{\partial v}{\partial x}\right), \;\; \tau_{yy} = \frac{\mu}{Re_\infty}\left(2\frac{\partial v}{\partial y} - \frac{2}{3}\left(\frac{\partial u}{\partial x} + \frac{\partial v}{\partial y}\right)\right)$$

$$q_x = \frac{-k}{(\gamma-1)M_\infty^2 Pr_\infty Re_\infty}\left(\frac{\partial T}{\partial x}\right), \qquad q_y = \frac{-k}{(\gamma-1)M_\infty^2 Pr_\infty Re_\infty}\left(\frac{\partial T}{\partial y}\right)$$

The total energy per unit volume is given as, $e = \frac{p}{\gamma-1} + \frac{\rho(u^2+v^2)}{2}$, and the equation of state is given by, $p = \frac{\rho T}{\gamma M_\infty^2}$. The laminar viscosity and thermal conductivity are determined using Sutherland's formula[13].

3 Solution Methodology

A schematic representation of an unstructured mesh consisting of triangular elements is shown in Figure 1. The notation 'i' represents the centroid of the finite volume, while 'v' denotes the vertices forming the volume. Unlike, conventional finite volume method, the SUP updates solution variables not only at cell centres, but also at cell vertices. Alternatively, SUP can be viewed as a cell-centered finite

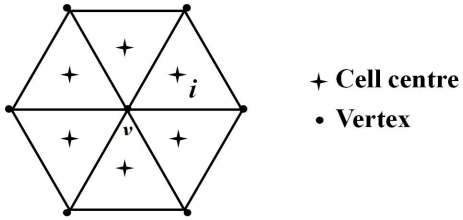

Figure 1: Stencil employed in SUP

volume procedure with a governing PDE based vertex value interpolation. The discretization details are explained in the following subsections.

3.1 Volume update

A cell-centred finite volume approach is employed for state update of finite volume. The computational domain is discretized into a set of non-overlapping control volumes and the conservation laws of mass, momentum and energy are integrated over these volumes. The state update for a finite volume i, as

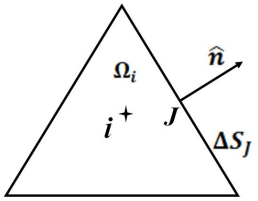

Figure 2: A typical finite volume

shown in Figure 2, obtained using single point quadrature can be expressed as,

$$\frac{\bar{\mathbf{w}}_i^{n+1} - \bar{\mathbf{w}}_i^n}{\Delta t} = -\frac{1}{\Omega_i} \sum_J \mathbf{f}_{\perp J} \Delta S_J \tag{2}$$

where $\mathbf{f}_{\perp J}$ is the total interfacial flux vector determined normal to the volume interface J.

3.2 Vertex update

In SUP framework, the flux derivatives at the cell vertex are obtained using a variant of Upwind-Least Squares Finite Difference (referred to as LSFD - U : Method II) [4, 14]; which is a generalized finite difference based technique that invariably employs method of least squares on a local cloud of points. A typical point cloud about vertex v is shown in Figure 3 with the neighbouring nodes denoted as w.

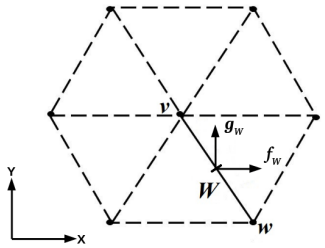

Figure 3: 2D cluster for LSFD – U : Method II

A mid-way fictitious interface W is introduced on the ray joining v and w. Using the method of least squares and assuming linear variation of fluxes between the node v and its neighbour w, the expressions

for flux derivatives can be represented in the form of matrix-vector equation as below:

$$\begin{aligned} \mathbf{G}\ \overrightarrow{\boldsymbol{\partial} f} &= \vec{\boldsymbol{\delta}}\,(\Delta f_{_W}) \\ \mathbf{G}\ \overrightarrow{\boldsymbol{\partial} g} &= \vec{\boldsymbol{\delta}}\,(\Delta g_{_W}) \end{aligned} \tag{3}$$

with the following definitions of the matrix and vectors,

$$\mathbf{G} = \begin{bmatrix} \sum\limits_{W} \Delta x_{_W}^2 & \sum\limits_{W} \Delta x_{_W} \Delta y_{_W} \\ \sum\limits_{W} \Delta x_{_W} \Delta y_{_W} & \sum\limits_{W} \Delta y_{_W}^2 \end{bmatrix}, \qquad \overrightarrow{\boldsymbol{\partial}(\cdot)} = \begin{bmatrix} (\cdot)_{x_v} \\ (\cdot)_{y_v} \end{bmatrix}, \qquad \vec{\boldsymbol{\delta}}\,(\cdot) = \begin{bmatrix} \sum\limits_{W} (\cdot)\,\Delta x_{_W} \\ \sum\limits_{W} (\cdot)\,\Delta y_{_W} \end{bmatrix}$$

Here, $\mathbf{G}$ is the geometric matrix resulting from 2-D linear least squares approximation, and $\Delta(\cdot)_{_W} = (\cdot)_{_W} - (\cdot)_v$. Note that, f and g are components of flux vectors, $\mathbf{f}$ and $\mathbf{g}$, respectively. Hence, the flux derivatives required for state update at v can be expressed as,

$$f_{x_v} = \sum_{l=1}^{2} G_{1,l}^{-1} \delta_l(\Delta f_{_W}) \qquad \text{and} \qquad g_{y_v} = \sum_{l=1}^{2} G_{2,l}^{-1} \delta_l(\Delta g_{_W}). \tag{4}$$

Referring to Figure 3, the fluxes at the fictitious interface, i.e., $f_{_W}$ and $g_{_W}$ are need to be evaluated in addition to the fluxes at vertex v.

3.3 Computation of convective fluxes

Within the framework of SUP, an upwind flux is computed along the tangential direction of the volume interface in addition to the normal upwind flux.

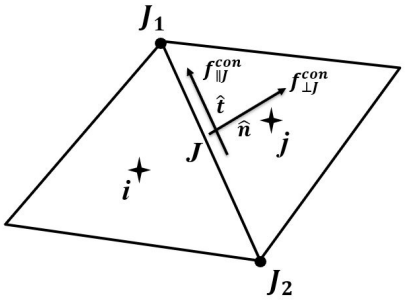

Figure 4: Upwind fluxes at a volume interface

For a given volume interface J as shown in Figure 4, i and j represent the left and right cells, respectively; J_1 and J_2 are the vertices forming the interface. Let $\hat{\boldsymbol{n}} = (n_x,\ n_y)$ and $\hat{\boldsymbol{t}} = (t_x,\ t_y)$ be the unit vectors normal and tangential to the interface J forming a right hand co-ordinate system, along which upwind fluxes are computed. In the present work, Roe's flux difference splitting scheme [15] is adopted for approximating both of the convective interfacial fluxes. Bringing in Roe's flux difference splitting scheme, the convective interfacial fluxes using appropriate extrapolated left and right states can be cast as below:

$$\begin{aligned} \mathbf{f}_{\perp J}^{con} &= \frac{1}{2}(\mathbf{f}_{\perp}^{con^+}(\phi_i^J) + \mathbf{f}_{\perp}^{con^-}(\phi_j^J)) - \frac{1}{2}\sum_k \alpha_{b_k} |\lambda_{b_k}| \vec{\boldsymbol{r}}_{b_k} \\ \mathbf{f}_{\parallel J}^{con} &= \frac{1}{2}\mathbf{f}_{\parallel}^{con^+}(\phi_{J_1}^J) + \mathbf{f}_{\parallel}^{con^-}(\phi_{J_2}^J) - \frac{1}{2}\sum_k \alpha_{b_k} |\lambda_{b_k}| \vec{\boldsymbol{r}}_{b_k} \end{aligned} \tag{5}$$

where, ϕ represents one of the primitive variables and $\phi_{(\cdot)}^J = \phi_{(\cdot)} + \boldsymbol{\nabla}\phi_{(\cdot)} \cdot \vec{\boldsymbol{r}}_{J(\cdot)}$, is the extrapolated state at volume interface. In above equation, α_{b_k} denotes the strength of k^{th} wave, λ_{b_k} represents the k^{th} eigenvalue of the Roe averaged matrix and $\vec{\boldsymbol{r}}_{b_k}$ denotes the corresponding eigenvector. The normal convective flux, $\mathbf{f}_{\perp J}^{con}$, directly goes into finite volume state update at cell centres. These higher order flux computations require solution gradients at cell centres as well as at cell vertices to represent the linear polynomial. In 2D, the upwind estimate of fluxes in these directions are available at W on the ray

joining v-w. The upwind flux vectors, $\mathbf{f}_{_W}^{^{con}}$ and $\mathbf{g}_{_W}^{^{con}}$, are obtained by making use of Equation (5):

$$\begin{aligned} \mathbf{f}_{_W}^{^{con}} &= \mathbf{f}_{\perp J}^{^{con}} n_x + \mathbf{f}_{\parallel J}^{^{con}} t_x \\ \mathbf{g}_{_W}^{^{con}} &= \mathbf{f}_{\perp J}^{^{con}} n_y + \mathbf{f}_{\parallel J}^{^{con}} t_y \end{aligned} \tag{6}$$

3.4 Computation of viscous fluxes

In finite volume method, the computation of viscous fluxes at volume interface require the interfacial velocity and temperature gradients. Concerning vertex update, the viscous flux derivatives, i.e., $f_{x_v}^{^{vis}}$ and $g_{y_v}^{^{vis}}$ are determined using the linear least squares based expressions provided in Equation (4). It can be appreciated that the LSFD-U procedure makes use of global stencil of grid points, thus, satisfying the elliptic nature of viscous fluxes. To sum up, the computation of viscous fluxes in SUP framework require gradients at volume interface as well as at vertices.

3.5 Gradient computation

In a typical finite volume procedure, employing linear reconstruction, and therefore requiring single point flux quadrature, the velocity gradients required for the computation of viscous fluxes at quadrature point, are obtained as volume averaged gradients over the covolume as shown in Figure 5 by using Green-Gauss procedure[8]. Consider any primitive variable, say ϕ, for which the discrete approximation of gradient

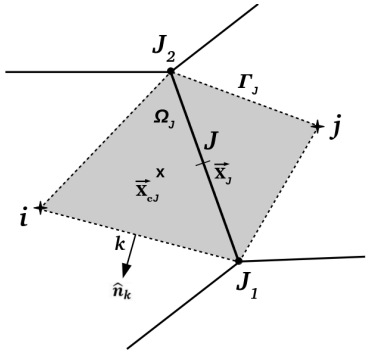

Figure 5: Covolume built around a volume interface

using single point quadrature can be expressed as,

$$\boldsymbol{\nabla}\phi_J^{^{num}} \simeq \frac{1}{\Omega_J} \sum_{k=1}^{4} \phi_k \hat{\boldsymbol{n}}_k \Delta S_k \tag{7}$$

where, ϕ_k is the value of solution variable at k^{th} quadrature point. Also, $\hat{\boldsymbol{n}}_k$ and ΔS_k represent the unit normal and length of the k^{th} edge of the covolume, respectively. Typically on an irregular grid, the solution gradients obtained are first order accurate at any point inside the covolume.

Our objective here is to compute viscous fluxes at volume interface to commensurate accuracy as that of convective fluxes obtained using a linear reconstruction procedure. This is achieved by the way of annihilating the $\mathcal{O}(h)$ leading error terms arising due to, (i) non-coincidence of the face centre, where the viscous fluxes are determined, with the centroid of the covolume, and (ii) use of single point quadrature. A defect corrected Green-Gauss procedure is proposed towards this goal. For a detailed discussion regarding the accuracy of Green-Gauss procedure and development of defect correction strategy, readers are referred to our report [9]. Only the essential steps are outlined here.

A defect corrected ϕ, i.e.,$\widetilde{\phi}_k$ is defined as:

$$\widetilde{\phi}_k = \dot{\phi}_k - \frac{1}{2}\left[\Delta\phi_{x_k}\overline{x}_k + \Delta\phi_{y_k}\overline{y}_k\right] \tag{8}$$

where, $\Delta\phi_{x_k} = \phi_{x_k} - \phi_{x_J}$ and $\Delta\phi_{y_k} = \phi_{y_k} - \phi_{y_J}$ with $\overline{x}_k = x_k - x_J$ and $\overline{y}_k = y_k - y_J$. Here, the notation $\dot{\phi}_k$ is the corrected value of the solution variable at the k^{th} quadrature point. The expression

for the same is given as:

$$\dot{\phi}_k = \frac{\dot{\phi}_1 + \dot{\phi}_2}{2} \tag{9}$$

where the solution values at the nodes consisting of a covolume edge are modified as following,

$$\dot{\phi}_1 = \phi_1 + \left.\frac{\partial \phi}{\partial s}\right|_1 \frac{\Delta S_k}{4} \quad ; \quad \dot{\phi}_2 = \phi_2 - \left.\frac{\partial \phi}{\partial s}\right|_2 \frac{\Delta S_k}{4}$$

where, $\left.\frac{\partial \phi}{\partial s}\right|_{1,2} = [(\nabla \phi)_{1,2} \cdot \hat{s}]$. Consequently, replacing ϕ_k by $\widetilde{\phi}_k$ in Equation (7) will result in second order accurate gradients at face centre within the framework provided by SUP while continuing to use single point quadrature, and is expressed as :

$$\nabla \phi_J^{(2)} \simeq \frac{1}{\Omega_J} \sum_{k=1}^{4} \widetilde{\phi}_k \hat{n}_k \Delta S_k \tag{10}$$

It is worth noting that the above correction is valid iff the gradients are recovered to second order accuracy both at volume centroid and vertex. In order to accomplish this, closed paths are identified around cell centre and vertex as shown in Figure 6 and are referred to as diamond path and petal path, respectively. The figures suggest that the paths involved in obtaining these gradients coincide with the path employed for face gradients. Hence, a face based procedure that simultaneously and recursively solves the three coupled defect correction strategies, is employed which recovers second order accurate gradients not only at volume interface, but also at centroids and vertices.

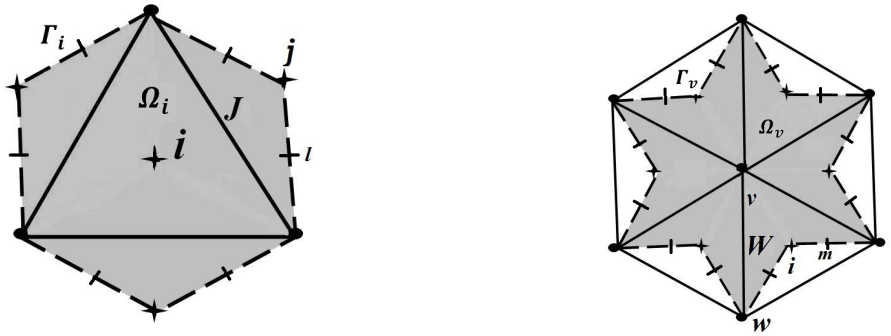

(a) Diamond path for cell centre

(b) Petal path for vertex

Figure 6: Closed paths for surface integration

These higher order accurate gradients are then used for linear solution reconstruction required for higher order convective flux computations as well as to compute viscous flux terms within SUP. The defect-corrected Green-Gauss procedure is iterative in nature and hence, computationally expensive. However, these additional computations can be effectively submerged by accelerating the solver using many core accelerator based processors. We have demonstrated the acceleration of the SUP solver by off-loading the gradient finding task onto GPU using OpenACC based programming model [16].

4 Results

An unsteady flow past a circular cylinder is investigated in this section. The test case corresponds to $M_\infty = 0.1$, $Re_\infty = 70$ (based on cylinder diameter, d) and $\alpha = 0°$. At this Re, a pair of alternate vortices are formed on the rear side of cylinder and are carried away with the surrounding main flow. This flow is simulated using an industry standard finite volume solver, HiFUN[1](High Resolution Flow

Table 1: Details of meshes around 2D circular cylinder

Mesh	N_p	N_c	N_w
Present study	10982	21732	200
Fine mesh	1984790	1980500	1000

Solver on Unstructured meshes) and SUP on a coarse triangulated mesh. Results are compared with fine grid solution obtained on a fine structured mesh using HiFUN. The mesh details are presented in Table 1. Different views of coarse mesh is shown in Figure 7.

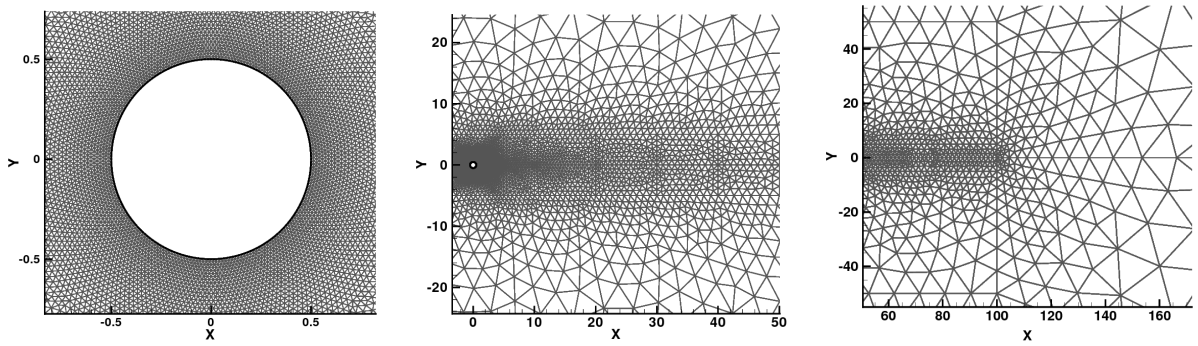

(a) Around cylinder (b) Near wake region (c) Far wake region

Figure 7: Views of mesh around circular cylinder in different regions of flow field

To perform the unsteady simulation, the dual time stepping procedure [17] based on second order accurate backward differencing is used for HiFUN simulations whereas the fourth order accurate explicit Runge-Kutta (RK4) time marching scheme is employed for SUP. The time step size used for all the simulations is set as $3.125\text{x}10^{-4}$.

The colour map of instantaneous Mach number contours in the wake region for all the simulations are presented in Figure 8. It is evident from these plots that there is significantly less diffusion in the wake obtained using SUP even on coarse mesh as compared to that of HiFUN solution on the same mesh. Additionally, at the same instance, the Z- vorticity contours are compared in Figure 9. On the given coarse mesh, the vortical structures from HiFUN diffuse earlier as compared to SUP. In other words, the vortex street, in case of SUP simulation, has additional length of $20d$.

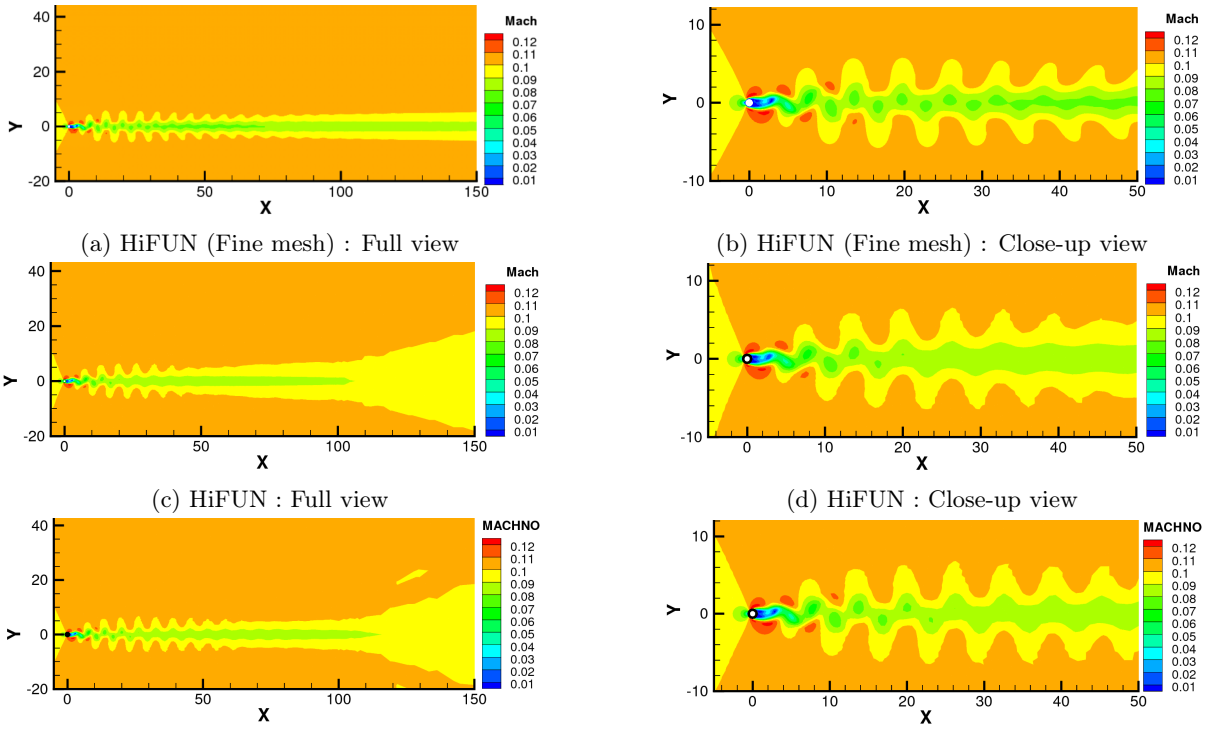

(a) HiFUN (Fine mesh) : Full view (b) HiFUN (Fine mesh) : Close-up view

(c) HiFUN : Full view (d) HiFUN : Close-up view

(e) SUP : Full view (f) SUP : Close-up view

Figure 8: Comparison of Mach number contours

[1] https://sandi.co.in/products/

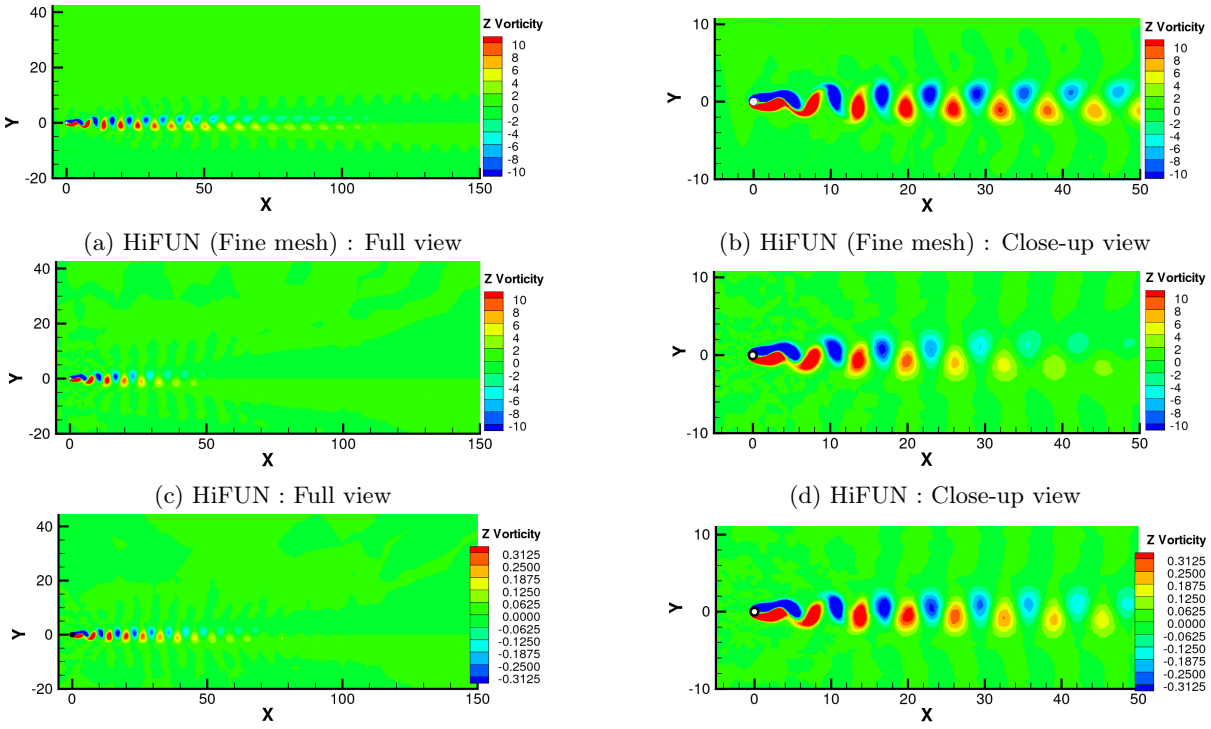

(a) HiFUN (Fine mesh) : Full view

(b) HiFUN (Fine mesh) : Close-up view

(c) HiFUN : Full view

(d) HiFUN : Close-up view

(e) SUP : Full view

(f) SUP : Close-up view

Figure 9: Comparison of Z- vorticity contours

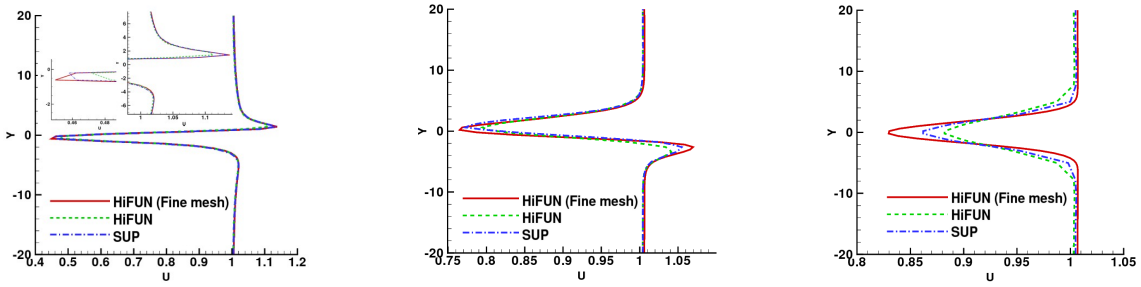

(a) At $x/d = 5$

(b) At $x/d = 20$

(c) At $x/d = 100$

Figure 10: Comparison of u velocity profiles at different stations in the wake

Figure 10 presents the comparison of streamwise velocity profiles across the wake at three different stations corresponding to $x/d = 5, 20$ and 100. Improvement in the prediction of wake deficit can be asserted in case of SUP as compared to that of HiFUN on the given mesh. In addition, the comparison of surface pressure and skin friction coefficient distribution over the cylinder surface are depicted in Figures 11 and 12, respectively. Better predictions are obtained with SUP.

The variation of integrated load coefficients, i.e., lift and drag coefficients with time for these unsteady simulations are presented in Figure 13. The c_l variation of SUP is in phase with that of fine grid solution. The St and time-averaged drag coefficients for all the simulations are provided in Table 2. The numbers predicted by SUP are closer to that of obtained on fine mesh using HiFUN.

Table 2: Summary of Strouhal number (St) and averaged drag coefficient

	$c_{d,avg}$	St
HiFUN	1.359	0.1426
SUP	1.364	0.1443
HiFUN (Fine mesh)	1.369	0.1445
Tritton [18]	-	0.1477

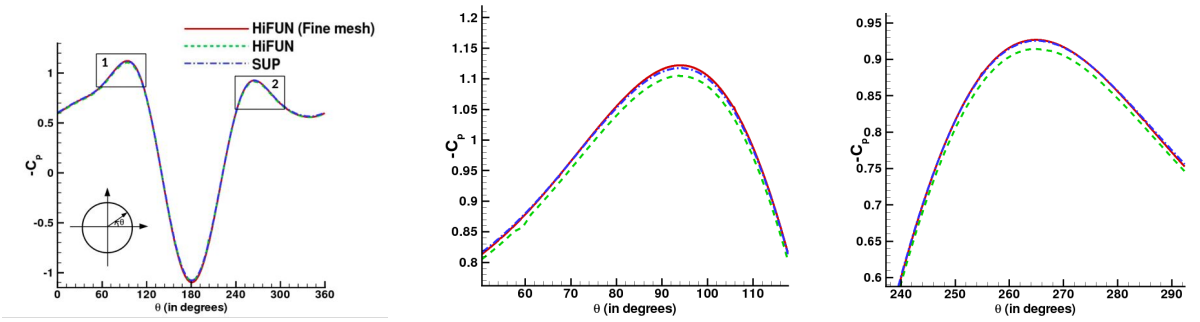

(a) Full view (b) View at Window 1 (c) View at Window 2

Figure 11: Comparison of surface pressure distribution

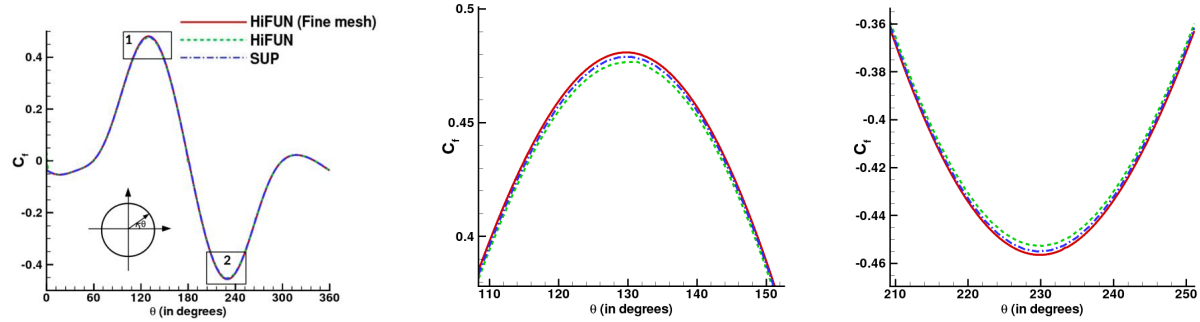

(a) Full view (b) View at Window 1 (c) View at Window 2

Figure 12: Comparison of skin friction coefficient distribution

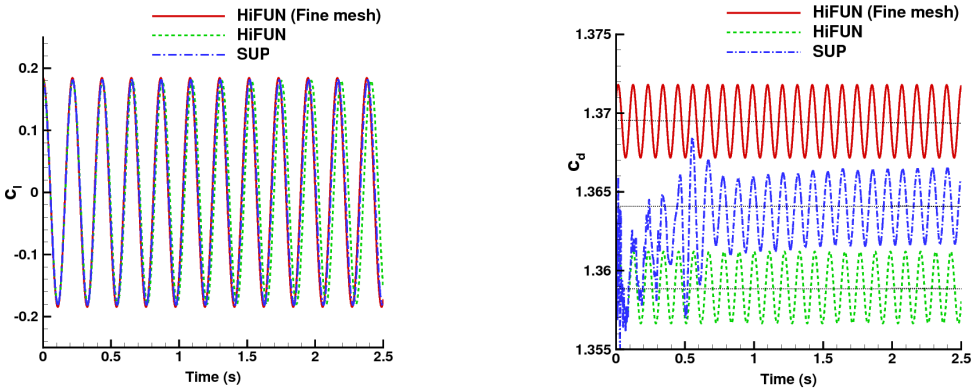

(a) c_l variation with time (b) c_d variation with time

Figure 13: Variation of integrated load coefficients

5 Conclusion and Future Work

The efficacy of the SUP methodology is established by solving an unsteady flow problem on a coarse triangulated mesh at a low Reynolds number. The improved solution accuracy and reduced numerical diffusion offered by SUP is encouraging and it shows lots of promise for p-adaptive DES calculations. In addition, our proposed methodology offers two significant advantages that are directly relevant to modern computer hardware. One of the important bottlenecks in the utilization of the processors comes from the latency associated with memory access. Compared to conventional finite volume schemes, our newly developed SUP algorithm operates more efficiently with the set of data accessed. This not only enhances the utilization of present-day processors but also improves solution accuracy. The second aspect pertains to the inherent data parallelism in the proposed methodology, which makes it naturally suitable for accelerating on the many core accelerator based processors such as GPUs.

Acknowledgments

The authors would like to express their gratitude to the Supercomputer Education and Research Centre (SERC), Indian Institute of Science, Bangalore, India, for providing the PARAMPravega supercomputing platform, which was extensively utilized for the HiFUN simulations referenced in this work. Additionally, we gratefully acknowledge the financial support provided by the Society for Innovation & Development (SID), Indian Institute of Science, Bangalore, India, for enabling our participation in this conference.

References

[1] Nikhil Shende and N Balakrishnan. Towards a Staggered Update Procedure for cell centre finite volume scheme. Technical report, *IISc AR&DB Fluid Mechanics Report FM02*, March 2001.

[2] Stephen F Davis. A rotationally biased upwind difference scheme for the Euler equations. *Journal of Computational Physics*, 56(1):65–92, 1984.

[3] D Sridar and N Balakrishnan. An upwind finite difference scheme for meshless solvers. *Journal of Computational Physics*, 189(1):1–29, 2003.

[4] N. Munikrishna. *On viscous flux discretization procedures for finite volume and meshless solvers.* PhD thesis, Indian Institute of Science, Bangalore, 2007.

[5] Carl Ollivier-Gooch and Michael Van Altena. A high-order-accurate unstructured mesh finite-volume scheme for the advection–diffusion equation. *Journal of Computational Physics*, 181(2):729–752, 2002.

[6] Alexandros Syrakos, Stylianos Varchanis, Yannis Dimakopoulos, Apostolos Goulas, and John Tsamopoulos. A critical analysis of some popular methods for the discretisation of the gradient operator in finite volume methods. *Physics of Fluids*, 29(12), 2017.

[7] Hiroaki Nishikawa. From hyperbolic diffusion scheme to gradient method: Implicit Green–Gauss gradients for unstructured grids. *Journal of Computational Physics*, 372:126–160, 2018.

[8] P Jawahar and Hemant Kamath. A high-resolution procedure for Euler and Navier–Stokes computations on unstructured grids. *Journal of Computational Physics*, 164(1):165–203, 2000.

[9] Shubhashree Subudhi and N Balakrishnan. Towards a Staggered Update Procedure (SUP) for Higher order Cell-centre Finite Volume Method II : Defect corrected gradients. Technical report, *CAd Lab Technical Note : CAd TN 2019:01* , May 2019.

[10] Shubhashree Subudhi and N Balakrishnan. A Staggered Update Procedure (SUP) for Higher-Order Cell-Centre Finite Volume Method. In *Proceedings of 16th Asian Congress of Fluid Mechanics*, pages 285–293. Springer, 2021.

[11] Shubhashree Subudhi and Balakrishnan Narayanarao. Two dimensional laminar flow computations on unstructured meshes using defect corrected Staggered Update Procedure. In *25th AIAA International Space Planes and Hypersonic Systems and Technologies Conference*, page 3058, 2023.

[12] Shubhashree Subudhi and Balakrishnan Narayanarao. Two dimensional Laminar flow computations using Staggered Update Procedure (SUP). In *Proceedings of the* 23^{rd} *Annual CFD Symposium of Aeronautical Society of India*, pages Bangalore, India, August 11-12, 2022.

[13] Herrmann Schlichting and Klaus Gersten. *Boundary-layer theory.* Springer Science & Business Media, 2003.

[14] Athaluri Gnana Kumar. “Variants of LSFD-U for compressible flows". Master’s thesis, Department of Aerospace Engineering, Indian Institute of Science, Bangalore, India, 2002.

[15] Philip L Roe. Approximate riemann solvers, parameter vectors, and difference schemes. *Journal of computational physics*, 43(2):357–372, 1981.

[16] Shubhashree Subudhi, Amol Khillare, N Munikrishna, and N Balakrishnan. GPU accelerated Staggered Update Procedure (SUP). *Submitted to Computers & Fluids, under review.*

[17] Antony Jameson. Time dependent calculations using multigrid, with applications to unsteady flows past airfoils and wings. In *10th Computational fluid dynamics conference*, page 1596, 1991.

[18] David J Tritton. Experiments on the flow past a circular cylinder at low reynolds numbers. *Journal of Fluid Mechanics*, 6(4):547–567, 1959.